

Referring Image Segmentation via Cross-Modal Progressive Comprehension

Shaofei Huang^{1,2*} Tianrui Hui^{1,2*} Si Liu^{3†} Guanbin Li⁴ Yunchao Wei⁵
 Jizhong Han^{1,2} Luoqi Liu⁶ Bo Li³

¹ Institute of Information Engineering, Chinese Academy of Sciences

² School of Cyber Security, University of Chinese Academy of Sciences

³ School of Computer Science and Engineering, Beihang University

⁴ Sun Yat-sen University ⁵ University of Technology Sydney ⁶ 360 AI Institute

Abstract

Referring image segmentation aims at segmenting the foreground masks of the entities that can well match the description given in the natural language expression. Previous approaches tackle this problem using implicit feature interaction and fusion between visual and linguistic modalities, but usually fail to explore informative words of the expression to well align features from the two modalities for accurately identifying the referred entity. In this paper, we propose a Cross-Modal Progressive Comprehension (CMPC) module and a Text-Guided Feature Exchange (TGFE) module to effectively address the challenging task. Concretely, the CMPC module first employs entity and attribute words to perceive all the related entities that might be considered by the expression. Then, the relational words are adopted to highlight the correct entity as well as suppress other irrelevant ones by multimodal graph reasoning. In addition to the CMPC module, we further leverage a simple yet effective TGFE module to integrate the reasoned multimodal features from different levels with the guidance of textual information. In this way, features from multi-levels could communicate with each other and be refined based on the textual context. We conduct extensive experiments on four popular referring segmentation benchmarks and achieve new state-of-the-art performances. Code is available at <https://github.com/spyfly/CMPC-Refseg>.

1. Introduction

As deep models have made significant progresses in vision or language tasks [31][26][18][12][39], fields combining them [37][28][50] have drawn great attention of researchers. In this paper, we focus on the *referring image segmentation* (RIS) problem whose goal is to segment the

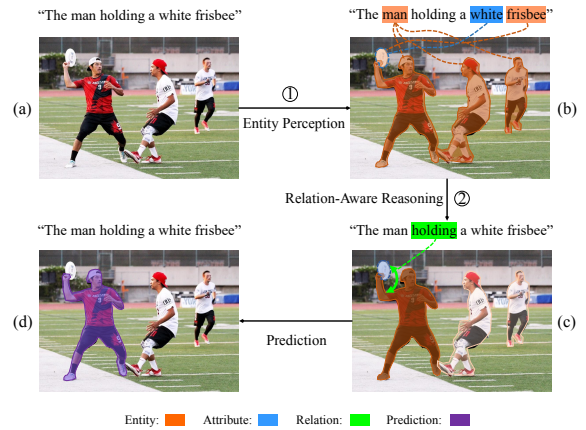


Figure 1. Interpretation of our progressive referring segmentation method. (a) Input referring expression and image. (b) The model first perceives all the entities described in the expression based on entity words and attribute words, e.g., “man” and “white frisbee” (orange masks and blue outline). (c) After finding out all the candidate entities that may match with input expression, relational word “holding” can be further exploited to highlight the entity involved with the relationship (green arrow) and suppress the others which are not involved. (d) Benefiting from the relation-aware reasoning process, the referred entity is found as the final prediction (purple mask). (Best viewed in color).

entities described by a natural language expression. Beyond traditional semantic segmentation, RIS is a more challenging problem since the expression can refer to *objects* or *stuff* belonging to any category in various language forms and contain diverse contents including entities, attributes and relationships. As a relatively new topic that is still far from being solved, this problem has a wide range of potential applications such as interactive image editing, language-based robot controlling, etc. Early works [17][30][34][23] tackle this problem using a straightforward concatenation-and-convolution scheme to fuse visual and linguistic features. Later works [38][3][44] further utilize inter-modality atten-

*Equal contribution

†Corresponding author

tion or self-attention to learn only visual embeddings or visual-textual co-embeddings for context modeling. However, these methods still lack the ability of exploiting different types of informative words in the expression to accurately align visual and linguistic features, which is crucial to the comprehension of both expression and image.

As illustrated in Figure 1 (a) and (b), if the referent, i.e., the entity referred to by the expression, is described by “The man holding a white frisbee”, a reasonable solution is to tackle the referring problem in a progressive way which can be divided into two stages. First, the model is supposed to perceive all the entities described in the expression according to entity words and attribute words, e.g., “man” and “white frisbee”. Second, as multiple entities of the same category may appear in one image, for example, the three men in Figure 1 (b), the model needs to further reason relationships among entities to highlight the referent and suppress the others that are not matched with the relationship cue given in the expression. In Figure 1 (c), the word “holding” which associates “man” with “white frisbee” powerfully guides the model to focus on the referent who holds a white frisbee rather than the other two men, which assists in making correct prediction in Figure 1 (d).

Based on the above motivation, we propose a Cross-Modal Progressive Comprehension (CMPC) module which progressively exploits different types of words in the expression to segment the referent in a graph-based structure. Concretely, our CMPC module consists of two stages. First, linguistic features of entity words and attribute words (e.g., “man” and “white frisbee”) extracted from the expression are fused with visual features extracted from the image to form multimodal features where all the entities considered by the expression are perceived. Second, we construct a fully-connected spatial graph where each vertex corresponds to an image region and feature of each vertex contains multimodal information of the entity. Vertices require appropriate edges to communicate with each other. Naive edges treating all the vertices equally will introduce abundant information and fail to distinguish the referent from other candidates. Therefore, our CMPC module employs relational words (e.g., “holding”) of the expression as a group of routers to build adaptive edges to connect spatial vertices, i.e., entities, that are involved with the relationship described in the expression. Particularly, spatial vertices (e.g., “man”) that have strong responses to the relational words (e.g., “holding”) will exchange information with others (e.g., “frisbee”) that also correlate with the relational words. Meanwhile, spatial vertices that have weak responses to the relational words will have less interaction with others. After relation-aware reasoning on the multimodal graph, feature of the referent can be highlighted while those of the irrelevant entities can be suppressed, which assists in generating accurate segmentation.

As multiple levels of features can complement each other [23][44][3], we also propose a Text-Guided Feature Exchange (TGFE) module to exploit information of multimodal features refined by our CMPC module from different levels. For each level of multimodal features, our TGFE module utilizes linguistic features as guidance to select useful feature channels from other levels to realize information communication. After multiple rounds of communication, multi-level features are further fused by ConvLSTM [42] to comprehensively integrate low-level visual details and high-level semantics for precise mask prediction.

Our contributions are summarized as follows: (1) We propose a Cross-Modal Progressive Comprehension (CMPC) module which first perceives all the entities that are possibly referred by the expression, then utilizes relationship cues of the input expression to highlight the referent while suppressing other irrelevant ones, yielding discriminative feature representations for the referent. (2) We also propose a Text-Guided Feature Exchange (TGFE) module to conduct adaptive information communication among multi-level features under the guidance of linguistic features, which further enhances feature representations for mask prediction. (3) Our method achieves new state-of-the-art results on four referring segmentation benchmarks, demonstrating the effectiveness of our model.

2. Related Work

2.1. Semantic Segmentation

Semantic segmentation has made a huge progress based on Fully Convolutional Networks (FCN) [32]. FCN replaces fully-connected layers in original classification networks with convolution layers and becomes the standard architecture of the following segmentation methods. DeepLab [4][5][6] introduces atrous convolution with different atrous rates into FCN model to enlarge the receptive field of filters and aggregate multi-scale context. PSPNet [49] utilizes pyramid pooling operations to extract multi-scale context as well. Recent works such as DANet [11] and CFNet [47] employ self-attention mechanism [40] to capture long-range dependencies in deep networks and achieve notable performance. In this paper, we tackle the more generalized and challenging semantic segmentation problem whose semantic categories are specified by natural language referring expression.

2.2. Referring Expression Comprehension

The goal of referring expression comprehension is to localize the entities in the image which are matched with the description of a natural language expression. Many works conduct localization in bounding box level. Liao *et al.* [27] performs cross-modality correlation filtering to match multimodal features in real time. Relationships between vision and language modalities [16][43] are also modeled to match

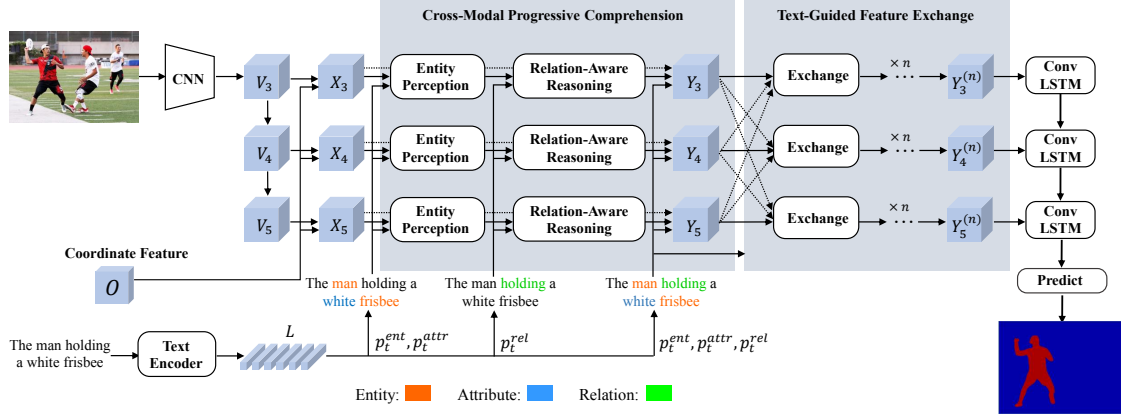


Figure 2. Overview of our proposed method. Visual features and linguistic features are first progressively aligned by our Cross-Modal Progressive Comprehension (CMPC) module. Then multi-level multimodal features are fed into our Text-Guided Feature Exchange (TGFE) module for information communication across different levels. Finally, multi-level features are fused with ConvLSTM for final prediction.

the expression with most related objects. Modular networks are explored in [45] to decompose the referring expression into subject, location and relationship so that the matching score is more finely computed.

Beyond bounding box, the referred object can also be localized more precisely with segmentation mask. Hu *et al.* [17] first proposes the referring segmentation problem and generates the segmentation mask by directly concatenating and fusing multimodal features from CNN and LSTM [15]. In [30], multimodal LSTM is employed to sequentially fuse visual and linguistic features in multiple time steps. Based on [30], dynamic filters [34] for each word further enhance multimodal features. Fusing multi-level visual features is explored in [23] to recurrently refine the local details of segmentation mask. As context information is critical to segmentation task, Shi *et al.* [38] utilizes word attention to aggregate only visual context to enhance visual features. For multimodal context extraction, cross-modal self-attention is exploited in [44] to capture long-range dependencies between each image region and each referring word. Visual-textual co-embedding is explored in [3] to measure compatibility between referring expression and image. Adversarial learning [36] and cycle-consistency [8] between referring expression and its reconstructed caption are also investigated to boost the segmentation performance. In this paper, we propose to progressively highlight the referent via entity perception and relation-aware reasoning for accurate referring segmentation.

2.3. Graph-Based Reasoning

It has been shown that graph-based models are effective for context reasoning in many tasks. Dense CRF [2] is a widely used graph model for post-processing in image segmentation. Recently, Graph Convolution Networks (GCN) [2] becomes popular for its superiority on semi-

supervised classification. Wang *et al.* [41] construct a spatial-temporal graph using region proposals as vertexes and conduct context reasoning with GCN, which performs well on video recognition task. Chen *et al.* [7] propose a global reasoning module which projects visual feature into an interactive space and conducts graph convolution for global context reasoning. The reasoned global context is projected back to the coordinate space to enhance original visual feature. There are several concurrent works [24][25][48] sharing the same idea of projection and graph reasoning with different implementation details. In this paper, we propose to regard image regions as vertexes to build a spatial graph where each vertex saves multimodal feature vector as its state. Information flow among vertexes is routed by relational words in the referring expression and implemented using graph convolution. After the graph reasoning, image regions can generate accurate and coherent responses to the referring expression.

3. Method

Given an image and a natural language expression, the goal of our model is to segment the corresponding entity referred to by the expression, i.e., the referent. The overall architecture of our model is illustrated in Figure 2. We first extract the visual features of the image with a CNN backbone and the linguistic features of the expression with a text encoder. A novel Cross-Modal Progressive Comprehension (CMPC) module is proposed to progressively highlight the referent and suppress the others via entity perception and subsequent relation-aware reasoning on spatial region graph. The proposed CMPC module is applied to multiple levels of visual features respectively and the corresponding outputs are fed into a Text-Guided Feature Exchange (TGFE) module to communicate information under the guidance of linguistic modality. After the communi-

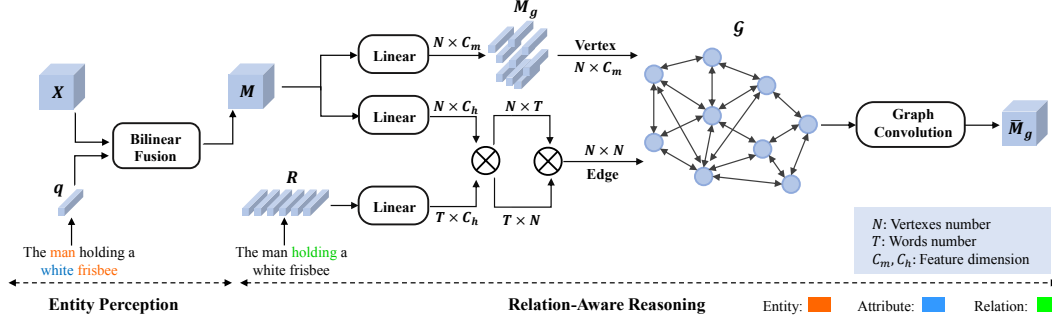


Figure 3. Illustration of our Cross-Modal Progressive Comprehension module which consists of two stages. First, visual features X are bilinearly fused with linguistic features q of entity words and attribute words for Entity Perception (EP) stage. Second, multimodal features M from EP stage are fed into Relation-Aware Reasoning (RAR) stage for feature enhancement. A multimodal fully-connected graph \mathcal{G} is constructed with each vertex corresponds to an image region on M . The adjacency matrix of \mathcal{G} is defined as the product of the matching degrees between vertexes and relational words in the expression. Graph convolution is utilized to reason among vertexes so that the referent could be highlighted during the interaction with correlated vertexes.

cation, multi-level features are finally fused with ConvLSTM [42] to make the prediction. We will elaborate each part of our method in the rest subsections.

3.1. Visual and Linguistic Feature Extraction

As shown in Figure 2, our model takes an image and an expression as inputs. The multi-level visual features are extracted with a CNN backbone and respectively fused with an 8-D spatial coordinate feature $O \in \mathbb{R}^{H \times W \times 8}$ using a 1×1 convolution following prior works [30][44]. After the convolution, each level of visual features are transformed to the same size of $\mathbb{R}^{H \times W \times C_v}$, with H , W and C_v being the height, width and channel dimension of the visual features. The transformed visual features are denoted as $\{X_3, X_4, X_5\}$ corresponding to the output of the 3rd, 4th and 5th stages of CNN backbone (e.g., ResNet-101 [14]). For ease of presentation, we denote a single level of visual features as X in Sec. 3.2. The linguistic features $L = \{l_1, l_2, \dots, l_T\}$ is extracted with a language encoder (e.g., LSTM [15]), where T is the length of expression and $l_i \in \mathbb{R}^{C_l}$ ($i \in \{1, 2, \dots, T\}$) denotes feature of the i -th word.

3.2. Cross-Modal Progressive Comprehension

As many entities may exist in the image, it is natural to progressively narrow down the candidate set from all the entities to the actual referent. In this section, we propose a Cross-Modal Progressive Comprehension (CMPC) module which consists of two stages, as illustrated in Figure 3. The first stage is entity perception. We associate linguistic features of entity words and attribute words with the correlated visual features of spatial regions using bilinear fusion [1] to obtain the multimodal features $M \in \mathbb{R}^{H \times W \times C_m}$. All the candidate entities are perceived by the fusion. The second stage is relation-aware reasoning. A fully-connected multimodal graph is constructed over M with relational words serving as a group of routers to connect vertexes. Each

vertex of the graph represents a spatial region on M . By reasoning among vertexes of the multimodal graph, the responses of the referent matched with the relationship cue are highlighted while those of non-referred ones are suppressed accordingly. Finally, the enhanced multimodal features \bar{M}_g are further fused with visual and linguistic features.

Entity Perception. Similar to [43], we classify the words into 4 types, including entity, attribute, relation and unnecessary word. A 4-D vector is predicted for each word to indicate the probability of it being the four types respectively. We denote the probability vector for word t as $p_t = [p_t^{ent}, p_t^{attr}, p_t^{rel}, p_t^{un}] \in \mathbb{R}^4$ and calculate it as:

$$p_t = \text{softmax}(W_2 \sigma(W_1 l_t + b_1) + b_2), \quad (1)$$

where $W_1 \in \mathbb{R}^{C_n \times C_l}$, $W_2 \in \mathbb{R}^{4 \times C_n}$, $b_1 \in \mathbb{R}^{C_n}$ and $b_2 \in \mathbb{R}^4$ are learnable parameters, $\sigma(\cdot)$ is sigmoid function, p_t^{ent} , p_t^{attr} , p_t^{rel} and p_t^{un} denote the probabilities of word t being the entity, attribute, relation and unnecessary word respectively. Then the global language context of entities $q \in \mathbb{R}^{C_l}$ could be calculated as a weighted combination of the all the words in the expression:

$$q = \sum_{t=1}^T (p_t^{ent} + p_t^{attr}) l_t. \quad (2)$$

Next, we adopt a simplified bilinear fusion strategy [1] to associate q with the visual feature of each spatial region:

$$M_i = (q W_{3i}) \odot (X W_{4i}), \quad (3)$$

$$M = \sum_{i=1}^r M_i \quad (4)$$

where $W_{3i} \in \mathbb{R}^{C_l \times C_m}$ and $W_{4i} \in \mathbb{R}^{C_v \times C_m}$ are learnable parameters, r is a hyper-parameter and \odot denotes element-

wise product. By integrating both visual and linguistic context into the multimodal features, all the entities that might be referred to by the expression are perceived appropriately.

Relation-Aware Reasoning. To selectively highlight the referent, we construct a fully-connected graph over the multimodal features M and conduct reasoning over the graph according to relational cues in the expression. Formally, the multimodal graph is defined as $\mathcal{G} = (\mathcal{V}, \mathcal{E}, M_g, A)$ where \mathcal{V} and \mathcal{E} are the sets of vertexes and edges, $M_g = \{m_i\}_{i=1}^N \in \mathbb{R}^{N \times C_m}$ is the set of vertex features, $A \in \mathbb{R}^{N \times N}$ is the adjacency matrix and N is number of vertexes.

Details of relation-aware reasoning is illustrated in the right part of Figure 3. As each location on M represents a spatial region on the original image, we regard each region as a vertex of the graph and the multimodal graph is composed of $N = H \times W$ vertexes in total. After the reshaping operation, a linear layer is applied to M to transform it into the features of vertexes M_g . The edge weights depend on the affinities between vertexes and relational words in the referring expression. Features of relational words $R = \{r_t\}_{t=1}^T \in \mathbb{R}^{T \times C_l}$ are calculated as:

$$r_t = p_t^{rel} l_t, \quad t = 1, 2, \dots, T. \quad (5)$$

As shown in Figure 3, adjacency matrix A is formulated as:

$$B = (M_g W_5)(R W_6)^T, \quad (6)$$

$$B_1 = \text{softmax}(B), \quad (7)$$

$$B_2 = \text{softmax}(B^T), \quad (8)$$

$$A = B_1 B_2, \quad (9)$$

where $W_5 \in \mathbb{R}^{C_m \times C_h}$ and $W_6 \in \mathbb{R}^{C_l \times C_h}$ are learnable parameters. $B \in \mathbb{R}^{N \times T}$ is the affinity matrix between M_g and R . We apply the softmax function along the second and first dimension of B to obtain $B_1 \in \mathbb{R}^{N \times T}$ and $B_2 \in \mathbb{R}^{T \times N}$ respectively. A is obtained by matrix product of B_1 and B_2 . Each element A_{ij} of A represents the normalized magnitude of information flow from the spatial region i to the region j , which depends on their affinities with relational words in the expression. In this way, relational words of the expression can be leveraged as a group of routers to build adaptive edges connecting vertexes.

After the construction of multimodal graph \mathcal{G} , we apply graph convolution [21] to it as follow:

$$\bar{M}_g = (A + I)M_g W_7, \quad (10)$$

where $W_7 \in \mathbb{R}^{C_m \times C_m}$ is a learnable weight matrix. I is identity matrix serving as a shortcut to ease optimization. The graph convolution reasons among vertexes, i.e., image regions, so that the referent is selectively highlighted according to the relationship cues while other irrelevant ones are suppressed, which assists in generating more discriminative feature representations for referring segmentation.

Afterwards, reshaping operation is applied to obtain the enhanced multimodal features $\bar{M}_g \in \mathbb{R}^{H \times W \times C_m}$. To incorporate the textual information, we first combine features of all necessary words into a vector $s \in \mathbb{R}^{C_l}$ with the pre-defined probability vectors:

$$s = \sum_{t=0}^T (p_t^{ent} + p_t^{attr} + p_t^{rel}) l_t. \quad (11)$$

We repeat s for $H \times W$ times and concatenate it with X and \bar{M}_g along channel dimension following with a 1×1 convolution to get the output features $Y \in \mathbb{R}^{H \times W \times C_m}$, which is equipped with multimodal context for the referent.

3.3. Text-Guided Feature Exchange

As previous works [23][44] show that multi-level semantics are essential to referring segmentation, we further introduce a Text-Guided Feature Exchange (TGFE) module to communicate information among multi-level features based on the visual and language context. As illustrated in Figure 2, the TGFE module takes Y_3, Y_4, Y_5 and word features $[l_1, l_2, \dots, l_T]$ as input. After n rounds of feature exchange, $Y_3^{(n)}, Y_4^{(n)}, Y_5^{(n)}$ are produced as outputs.

To get $Y_i^{(k)}$, $i \in \{3, 4, 5\}, k \geq 1$, we first extract a global vector $g_i^{(k-1)} \in \mathbb{R}^{C_m}$ of $Y_i^{(k-1)}$ by weighted global pooling:

$$g_i^{(k-1)} = \Lambda_i^{(k-1)} Y_i^{(k-1)}, \quad (12)$$

where the weight matrix $\Lambda_i^{(k-1)} \in \mathbb{R}^{H \times W}$ is derived from:

$$\Lambda_i^{(k-1)} = (s W_8)(Y_i^{(k-1)} W_9)^T, \quad (13)$$

where $W_8 \in \mathbb{R}^{C_l \times C_h}$ and $W_9 \in \mathbb{R}^{C_m \times C_h}$ are transforming matrices. Then a context vector $c_i^{(k-1)}$ which contains multimodal context of $Y_i^{(k-1)}$ is calculated by fusing s and $g_i^{(k-1)}$ with a fully connected layer. We finally select information correlated with level i from features of other two levels to form the refined features of level i at round k :

$$Y_i^{(k)} = \begin{cases} Y_i^{(k-1)} + \sum_{j \in \{3, 4, 5\} \setminus \{i\}} \sigma(c_i^{(k-1)}) \odot Y_j^{(k-1)}, & k \geq 1 \\ Y_i, & k = 0 \end{cases} \quad (14)$$

where $\sigma(\cdot)$ denotes the sigmoid function. After n rounds of feature exchange, features of each level are mutually refined to fit the context referred to by the expression. We further fuse the output features $Y_3^{(n)}, Y_4^{(n)}$ and $Y_5^{(n)}$ with ConvLSTM [42] for harvesting the final prediction.

4. Experiments

4.1. Experimental Setup

Datasets. We conduct extensive experiments on four benchmark datasets for referring image segmentation in-

| Method | UNC | | | UNC+ | | | G-Ref | ReferIt |
|---------------|--------------|--------------|--------------|--------------|--------------|--------------|--------------|--------------|
| | val | testA | testB | val | testA | testB | val | test |
| LSTM-CNN [17] | - | - | - | - | - | - | 28.14 | 48.03 |
| RMI [30] | 45.18 | 45.69 | 45.57 | 29.86 | 30.48 | 29.50 | 34.52 | 58.73 |
| DMN [34] | 49.78 | 54.83 | 45.13 | 38.88 | 44.22 | 32.29 | 36.76 | 52.81 |
| KWA [38] | - | - | - | - | - | - | 36.92 | 59.09 |
| ASGN [36] | 50.46 | 51.20 | 49.27 | 38.41 | 39.79 | 35.97 | 41.36 | 60.31 |
| RRN [23] | 55.33 | 57.26 | 53.95 | 39.75 | 42.15 | 36.11 | 36.45 | 63.63 |
| MAttNet [45] | 56.51 | 62.37 | 51.70 | 46.67 | 52.39 | 40.08 | n/a | - |
| CMSA [44] | 58.32 | 60.61 | 55.09 | 43.76 | 47.60 | 37.89 | 39.98 | 63.80 |
| CAC [8] | 58.90 | 61.77 | 53.81 | - | - | - | 44.32 | - |
| STEP [3] | 60.04 | 63.46 | 57.97 | 48.19 | 52.33 | 40.41 | 46.40 | 64.13 |
| Ours | 61.36 | 64.53 | 59.64 | 49.56 | 53.44 | 43.23 | 49.05 | 65.53 |

Table 1. Comparison with state-of-the-art methods on four benchmark datasets using *overall IoU* as metric. “n/a” denotes MAttNet does not use the same split as other methods.

cluding UNC [46], UNC+ [46], G-Ref [33] and ReferIt [19].

UNC, UNC+ and G-Ref datasets are all collected based on MS-COCO [29]. They contain 19,994, 19,992 and 26,711 images with 142,209, 141,564 and 104,560 referring expressions for over 50,000 objects, respectively. UNC+ has no location words and G-Ref contains much longer sentences (average length of 8.4 words) than others (less than 4 words), making them more challenging than UNC dataset. ReferIt dataset is collected on IAPR TC-12 [9] and contains 19,894 images with 130,525 expressions for 96,654 objects (including stuff).

Implementation Details. We adopt DeepLab-101 [5] pretrained on PASCAL-VOC dataset [10] as the CNN backbone following prior works [44][23] and use the output of Res3, Res4 and Res5 for multi-level feature fusion. Input images are resized to 320×320 . Channel dimensions of features are set as $C_v = C_l = C_m = C_h = 1000$ and the cell size of ConvLSTM [42] is set to 500. When comparing with other methods, the hyper-parameter r of bilinear fusion is set to 5 and the number of feature exchange rounds n is set to 3. GloVe word embeddings [35] pretrained on Common Crawl 840B tokens are adopted following [3]. Number of graph convolution layers is set to 2 on G-Ref dataset and 1 on others. The network is trained using Adam optimizer [20] with the initial learning rate of $2.5e^{-4}$ and weight decay of $5e^{-4}$. Parameters of CNN backbone are fixed during training. The standard binary cross-entropy loss averaged over all pixels is leveraged for training. For fair comparison with prior works, DenseCRF [22] is adopted to refine the segmentation masks.

Evaluation Metrics. Following prior works [17][44][3], overall Intersection-over-Union (Overall IoU) and Prec@X are adopted as metrics to evaluate our model. Overall IoU calculates total intersection regions over total union regions of all the test samples. Prec@X measures the percentage of predictions whose IoU are higher than the threshold X with $X \in \{0.5, 0.6, 0.7, 0.8, 0.9\}$.

4.2. Comparison with State-of-the-arts

To demonstrate the superiority of our method, we evaluate it on four referring segmentation benchmarks. Comparison results are presented in Table 1. We follow prior works [44][3] to only report overall IoU due to the limit of pages. Full results are included in supplementary materials. As illustrated in Table 1, our method outperforms all the previous state-of-the-arts on four benchmarks with large margins. Comparing with STEP [3] which densely fuses 5 levels of features for 25 times, our method exploits fewer levels of features and fusion times while consistently achieving 1.40%-2.82% performance gains on all the four datasets, demonstrating the effectiveness of our modules. In particular, our method yields 2.65% IoU boost against STEP on G-Ref val set, indicating that our method could better handle long sentences than those lack the ability of progressive comprehension. Besides, ReferIt is a challenging dataset and previous methods only have marginal improvements on it. For example, STEP and CMSA [44] obtain only 0.33% and 0.17% improvements on ReferIt test set respectively, while our method enlarges the performance gain to 1.40%, which shows that our model can well generalize to multiple datasets with different characteristics. In addition, our method also outperforms MAttNet [45] by a large margin in Overall IoU. Though MAttNet achieves higher precisions (e.g., 75.16% versus 71.72% in Prec@0.5 on UNC val set) than ours, it relies on Mask R-CNN [13] pretrained on noticeably more COCO [29] images (110K) than ours pretrained on PASCAL-VOC [10] images (10K). Therefore, it may not be completely fair to directly compare performances of MAttNet with ours.

4.3. Ablation Studies

We perform ablation studies on UNC val set and G-Ref val set to testify the effectiveness of each proposed module.

Components of CMPC Module. We first explore the

| | EP | RAR | TGFE | GloVe | Prec@0.5 | Prec@0.6 | Prec@0.7 | Prec@0.8 | Prec@0.9 | Overall IoU |
|----|----|-----|------|-------|--------------|--------------|--------------|--------------|--------------|--------------|
| 1 | | | | | 48.01 | 37.98 | 27.92 | 16.30 | 3.72 | 47.36 |
| 2 | ✓ | | | | 49.76 | 40.35 | 30.15 | 17.84 | 4.16 | 49.06 |
| 3 | | ✓ | | | 59.32 | 51.16 | 40.59 | 26.50 | 6.66 | 53.40 |
| 4 | ✓ | ✓ | | | 62.86 | 54.54 | 44.10 | 28.65 | 7.24 | 55.38 |
| 5 | ✓ | ✓ | | ✓ | 62.87 | 54.91 | 44.16 | 28.43 | 7.23 | 56.00 |
| 6* | | | | | 63.12 | 54.56 | 44.20 | 28.75 | 8.51 | 56.38 |
| 7 | | | ✓ | | 67.63 | 59.80 | 49.72 | 34.45 | 10.62 | 58.81 |
| 8 | ✓ | | ✓ | | 68.39 | 60.92 | 50.70 | 35.24 | 11.13 | 59.05 |
| 9 | | ✓ | ✓ | | 69.37 | 62.28 | 52.66 | 36.89 | 11.27 | 59.62 |
| 10 | ✓ | ✓ | ✓ | | 71.04 | 64.02 | 54.25 | 38.45 | 11.99 | 60.72 |
| 11 | ✓ | ✓ | ✓ | ✓ | 71.27 | 64.44 | 55.03 | 39.28 | 12.89 | 61.19 |

Table 2. Ablation studies on UNC val set. *Row 6 is the multi-level version of row 1 using only ConvLSTM for fusion. EP and RAR indicate entity perception stage and relation-aware reasoning stage in our CMPC module respectively.

effectiveness of each component of our proposed CMPC module and the experimental results are shown in Table 2. EP and RAR denotes the entity perception stage and relation-aware reasoning stage in CMPC module respectively. GloVe means using GloVe word embeddings [35] to initialize the embedding layer, which is also adopted in [3]. Results of rows 1 to 5 are all based on single-level features, i.e. Res5. Our baseline is implemented as simply concatenating the visual feature extracted with DeepLab-101 and linguistic feature extracted with an LSTM and making prediction on the fusion of them. As shown in row 2 of Table 2, including EP brings 1.70% IoU improvement over the baseline, indicating the perception of candidate entities are essential to the feature alignment between visual and linguistic modalities. In row 3, RAR alone brings 6.04% IoU improvement over baseline, which demonstrates that leveraging relational words as routers to reason among spatial regions could effectively highlight the referent in the image, thus boosting the performance notably. Combining EP with RAR, as shown in row 4, our CMPC module could achieve 55.38% IoU with single level features, outperforming baseline with a large margin of 8.02% IoU. This indicates that our model could accurately identity the referent by progressively comprehending the expression and image. Integrated with GloVe word embeddings, the IoU gain further achieves 8.64% with the aid of large-scale corpus.

We further conduct ablation studies based on multi-level features in rows 6 to 11 of Table 2. Row 6 is the multi-level version of row 1 using ConvLSTM to fuse multi-level features. The TGFE module in rows 7 to 11 is based on single round of feature exchange. As shown in Table 2, our model performs consistently with the single level version, which well proves the effectiveness of our CMPC module.

TGFE module. Table 3 presents the ablation results of TGFE module. n is the number of feature exchange rounds. The experiments are based on multi-level features with CMPC module. It is shown that only one round of feature exchange in TGFE could improve the IoU from 59.85%

to 60.72%. When we increase the rounds of feature exchange in TGFE, the IoU increases as well, which well proves the effectiveness of our TGFE module. We further evaluate TGFE module on baseline model and the comparing results are shown in row 6 and row 7 of Table 2. TGFE with single round of feature exchange improves the IoU from 56.38% to 58.81%, indicating that our TGFE module can effectively utilize rich contexts in multi-level features.

| CMPC only | +TGFE | | |
|-----------|---------|---------|--------------|
| | $n = 1$ | $n = 2$ | $n = 3$ |
| 59.85 | 60.72 | 61.07 | 61.25 |

Table 3. Overall IoUs of different numbers of feature exchange rounds in TGFE module on UNC val set. n denotes the number of feature exchange rounds.

| Dataset | CMPC | | | |
|-----------|---------|--------------|--------------|---------|
| | $n = 0$ | $n = 1$ | $n = 2$ | $n = 3$ |
| UNC val | 49.06 | 55.38 | 51.57 | 50.70 |
| G-Ref val | 36.50 | 38.19 | 40.12 | 38.96 |

Table 4. Experiments of graph convolution on UNC val set and G-Ref val set in terms of *overall IoU*. n denotes the number of graph convolution layers in our CMPC module. Experiments are all conducted on single level features.

Number of Graph Convolution Layer. In Table 4, we explore the number of graph convolution layers in CMPC module based on single-level features. n is the number of graph convolution layers in CMPC. Results on UNC val set show that more graph convolution layers leads to performance degradation. However, on G-Ref val set, 2 layers of graph convolution in CMPC achieves better performance than 1 layer while 3 layers decreasing the performance. As the average length of expressions in G-Ref (8.4 words) is much longer than that of UNC (< 4 words), we suppose that stacking more graph convolution layers in CMPC can appropriately improve the reasoning effect for longer referring expressions. However, too many graph convolution layers may introduce noises and harm the performance.

Qualitative Results. We presents qualitative comparison between the multi-level baseline model and our full

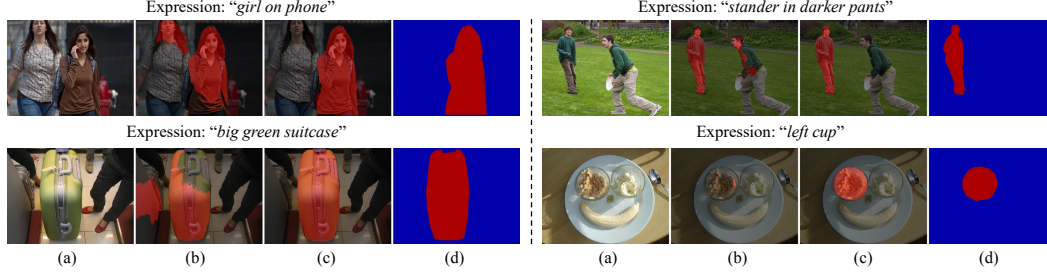


Figure 4. Qualitative results of referring image segmentation. (a) Original image. (b) Results predicted by the multi-level baseline model (row 6 in Table 2). (c) Results predicted by our full model (row 11 in Table 2). (d) Ground-truth.

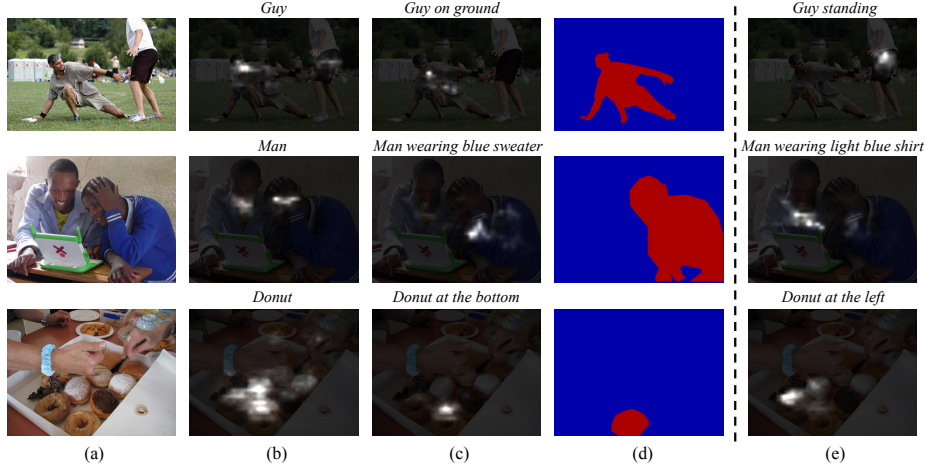


Figure 5. Visualization of affinity maps between images and expressions in our model. (a) Original image. (b)(c) Affinity maps of only entity words and full expressions in the test samples. (d) Ground-truth. (e) Affinity maps of expressions manually modified by us.

model in Figure 4. From the top-left example we can observe that the baseline model fails to make clear judgement between the two girls, while our full model is able to distinguish the correct girl having relationship with the phone, indicating the effectiveness of our CMPC module. Similar result is shown in the top-right example of Figure 4. As illustrated in the bottom row of Figure 4, attributes and location relationship can also be well handled by our full model.

Visualization of Affinity Maps. We visualize the affinity maps between multimodal feature and the first word in the expression in Figure 5. As shown in (b) and (c), our model is able to progressively produce more concentrated responses on the referent as the expression becomes more informative from only entity words to the full sentence. Interestingly, when we manually modify the expression to refer to other entities in the image, our model is still able to correctly comprehend the new expression and identify the referent. For example, in the third row of Figure 5(e), when the expression changes from “Donut at the bottom” to “Donut at the left”, high response area shifts from bottom donut to the left donut according to the expression. It indicates that our model can adapt to new expressions flexibly.

5. Conclusion and Future Work

To address the referring image segmentation problem, we propose a Cross-Modal Progressive Comprehension (CMPC) module which first perceives candidate entities considered by the expression using entity and attribute words, then conduct graph-based reasoning with the aid of relational words to further highlight the referent while suppressing others. We also propose a Text-Guided Feature Exchange (TGFE) module which exploits textual information to selectively integrate features from multiple levels to refine the mask prediction. Our model consistently outperforms previous state-of-the-art methods on four benchmarks, demonstrating its effectiveness. In the future, we plan to analyze the linguistic information more structurally and explore more compact graph formulation.

Acknowledgement This work was partially supported by the National Natural Science Foundation of China (Grant 61572493, Grant 61876177, Grant 61976250, Grant 61702565), Beijing Natural Science Foundation (L182013, 4202034), Fundamental Research Funds for the Central Universities and Zhejiang Lab (No. 2019KD0AB04).

References

- [1] Hedi Ben-Younes, Rémi Cadene, Matthieu Cord, and Nicolas Thome. Mutan: Multimodal tucker fusion for visual question answering. In *ICCV*, 2017.
- [2] Siddhartha Chandra, Nicolas Usunier, and Iasonas Kokkinos. Dense and low-rank gaussian crfs using deep embeddings. In *ICCV*, 2017.
- [3] Ding-Jie Chen, Songhao Jia, Yi-Chen Lo, Hwann-Tzong Chen, and Tyng-Luh Liu. See-through-text grouping for referring image segmentation. In *ICCV*, 2019.
- [4] Liang-Chieh Chen, George Papandreou, Iasonas Kokkinos, Kevin Murphy, and Alan L Yuille. Semantic image segmentation with deep convolutional nets and fully connected crfs. *arXiv preprint arXiv:1412.7062*, 2014.
- [5] Liang-Chieh Chen, George Papandreou, Iasonas Kokkinos, Kevin Murphy, and Alan L Yuille. Deeplab: Semantic image segmentation with deep convolutional nets, atrous convolution, and fully connected crfs. *TPAMI*, 2017.
- [6] Liang-Chieh Chen, George Papandreou, Florian Schroff, and Hartwig Adam. Rethinking atrous convolution for semantic image segmentation. *arXiv preprint arXiv:1706.05587*, 2017.
- [7] Yunpeng Chen, Marcus Rohrbach, Zhicheng Yan, Yan Shuicheng, Jiashi Feng, and Yannis Kalantidis. Graph-based global reasoning networks. In *CVPR*, 2019.
- [8] Yi-Wen Chen, Yi-Hsuan Tsai, Tiantian Wang, Yen-Yu Lin, and Ming-Hsuan Yang. Referring expression object segmentation with caption-aware consistency. *arXiv preprint arXiv:1910.04748*, 2019.
- [9] Hugo Jair Escalante, Carlos A Hernández, Jesus A Gonzalez, Aurelio López-López, Manuel Montes, Eduardo F Morales, L Enrique Sucar, Luis Villaseñor, and Michael Grubinger. The segmented and annotated iapr tc-12 benchmark. *CVIU*, 2010.
- [10] Mark Everingham, Luc Van Gool, Christopher KI Williams, John Winn, and Andrew Zisserman. The pascal visual object classes (voc) challenge. *IJCV*, 2010.
- [11] Jun Fu, Jing Liu, Haijie Tian, Yong Li, Yongjun Bao, Zhiwei Fang, and Hanqing Lu. Dual attention network for scene segmentation. In *CVPR*, 2019.
- [12] Chen Gao, Yunpeng Chen, Si Liu, Zhenxiong Tan, and Shuicheng Yan. Adversarialnas: Adversarial neural architecture search for gans. *arXiv preprint arXiv:1912.02037*, 2019.
- [13] Kaiming He, Georgia Gkioxari, Piotr Dollár, and Ross Girshick. Mask r-cnn. In *ICCV*, 2017.
- [14] Kaiming He, Xiangyu Zhang, Shaoqing Ren, and Jian Sun. Deep residual learning for image recognition. In *CVPR*, 2016.
- [15] Sepp Hochreiter and Jürgen Schmidhuber. Long short-term memory. *Neural Computation*, 1997.
- [16] Ronghang Hu, Marcus Rohrbach, Jacob Andreas, Trevor Darrell, and Kate Saenko. Modeling relationships in referential expressions with compositional modular networks. In *CVPR*, 2017.
- [17] Ronghang Hu, Marcus Rohrbach, and Trevor Darrell. Segmentation from natural language expressions. In *ECCV*, 2016.
- [18] Wentao Jiang, Si Liu, Chen Gao, Jie Cao, Ran He, Jiashi Feng, and Shuicheng Yan. Psgan: Pose and expression robust spatial-aware gan for customizable makeup transfer. *ArXiv*, abs/1909.06956, 2019.
- [19] Sahar Kazemzadeh, Vicente Ordonez, Mark Matten, and Tamara Berg. Referitgame: Referring to objects in photographs of natural scenes. In *EMNLP*, 2014.
- [20] Diederik P Kingma and Jimmy Ba. Adam: A method for stochastic optimization. *arXiv preprint arXiv:1412.6980*, 2014.
- [21] Thomas N Kipf and Max Welling. Semi-supervised classification with graph convolutional networks. *arXiv preprint arXiv:1609.02907*, 2016.
- [22] Philipp Krähenbühl and Vladlen Koltun. Efficient inference in fully connected crfs with gaussian edge potentials. In *NeurIPS*, 2011.
- [23] Ruiyu Li, Kaican Li, Yi-Chun Kuo, Michelle Shu, Xiaojuan Qi, Xiaoyong Shen, and Jiaya Jia. Referring image segmentation via recurrent refinement networks. In *CVPR*, 2018.
- [24] Yin Li and Abhinav Gupta. Beyond grids: Learning graph representations for visual recognition. In *NeurIPS*, 2018.
- [25] Xiaodan Liang, Zhiting Hu, Hao Zhang, Liang Lin, and Eric P Xing. Symbolic graph reasoning meets convolutions. In *NeurIPS*, 2018.
- [26] Yue Liao, Si Liu, Tianrui Hui, Chen Gao, Yao Sun, Hefei Ling, and Bo Li. Gps: Group people segmentation with detailed part inference. In *ICME*, 2019.
- [27] Yue Liao, Si Liu, Guanbin Li, Fei Wang, Yanjie Chen, Chen Qian, and Bo Li. A real-time cross-modality correlation filtering method for referring expression comprehension. *arXiv preprint arXiv:1909.07072*, 2019.
- [28] Yue Liao, Si Liu, Fei Wang, Yanjie Chen, Qian Chen, and Jiashi Feng. Ppdm: Parallel point detection and matching for real-time human-object interaction detection. *arXiv preprint arXiv:1912.12898*, 2019.
- [29] Tsung-Yi Lin, Michael Maire, Serge Belongie, James Hays, Pietro Perona, Deva Ramanan, Piotr Dollár, and C Lawrence Zitnick. Microsoft coco: Common objects in context. In *ECCV*, 2014.
- [30] Chenxi Liu, Zhe Lin, Xiaohui Shen, Jimei Yang, Xin Lu, and Alan Yuille. Recurrent multimodal interaction for referring image segmentation. In *ICCV*, 2017.
- [31] Si Liu, Guanghui Ren, Yao Sun, Jinqiao Wang, Changhu Wang, Bo Li, and Shuicheng Yan. Fine-grained human-centric tracklet segmentation with single frame supervision. *TPAMI*, 2020.
- [32] Jonathan Long, Evan Shelhamer, and Trevor Darrell. Fully convolutional networks for semantic segmentation. In *CVPR*, 2015.
- [33] Junhua Mao, Jonathan Huang, Alexander Toshev, Oana Camburu, Alan L Yuille, and Kevin Murphy. Generation and comprehension of unambiguous object descriptions. In *CVPR*, 2016.

- [34] Edgar Margffoy-Tuay, Juan C Pérez, Emilio Botero, and Pablo Arbeláez. Dynamic multimodal instance segmentation guided by natural language queries. In *ECCV*, 2018.
- [35] Jeffrey Pennington, Richard Socher, and Christopher D. Manning. Glove: Global vectors for word representation. In *EMNLP*, 2014.
- [36] Shuang Qiu, Yao Zhao, Jianbo Jiao, Yunchao Wei, and ShiKui Wei. Referring image segmentation by generative adversarial learning. *TMM*, 2019.
- [37] Guanghui Ren, Lejian Ren, Yue Liao, Si Liu, Bo Li, Jizhong Han, and Shuicheng Yan. Scene graph generation with hierarchical context. *TNNLS*, 2020.
- [38] Hengcan Shi, Hongliang Li, Fanman Meng, and Qingbo Wu. Key-word-aware network for referring expression image segmentation. In *ECCV*, 2018.
- [39] Ashish Vaswani, Noam Shazeer, Niki Parmar, Jakob Uszkoreit, Llion Jones, Aidan N Gomez, Łukasz Kaiser, and Illia Polosukhin. Attention is all you need. In *NeurIPS*, 2017.
- [40] Xiaolong Wang, Ross Girshick, Abhinav Gupta, and Kaiming He. Non-local neural networks. In *CVPR*, 2018.
- [41] Xiaolong Wang and Abhinav Gupta. Videos as space-time region graphs. In *ECCV*, 2018.
- [42] SHI Xingjian, Zhouong Chen, Hao Wang, Dit-Yan Yeung, Wai-Kin Wong, and Wang-chun Woo. Convolutional lstm network: A machine learning approach for precipitation nowcasting. In *NeurIPS*, 2015.
- [43] Sibe Yang, Guanbin Li, and Yizhou Yu. Cross-modal relationship inference for grounding referring expressions. In *CVPR*, 2019.
- [44] Linwei Ye, Mrigank Rochan, Zhi Liu, and Yang Wang. Cross-modal self-attention network for referring image segmentation. In *CVPR*, 2019.
- [45] Licheng Yu, Zhe Lin, Xiaohui Shen, Jimei Yang, Xin Lu, Mohit Bansal, and Tamara L Berg. MATTNet: Modular attention network for referring expression comprehension. In *CVPR*, 2018.
- [46] Licheng Yu, Patrick Poirson, Shan Yang, Alexander C Berg, and Tamara L Berg. Modeling context in referring expressions. In *ECCV*, 2016.
- [47] Hang Zhang, Han Zhang, Chenguang Wang, and Junyuan Xie. Co-occurrent features in semantic segmentation. In *CVPR*, 2019.
- [48] Songyang Zhang, Shipeng Yan, and Xuming He. Latentgcn: Learning efficient non-local relations for visual recognition. *arXiv preprint arXiv:1905.11634*, 2019.
- [49] Hengshuang Zhao, Jianping Shi, Xiaojuan Qi, Xiaogang Wang, and Jiaya Jia. Pyramid scene parsing network. In *CVPR*, 2017.
- [50] Zilong Zheng, Wenguan Wang, Siyuan Qi, and Song-Chun Zhu. Reasoning visual dialogs with structural and partial observations. In *CVPR*, 2019.